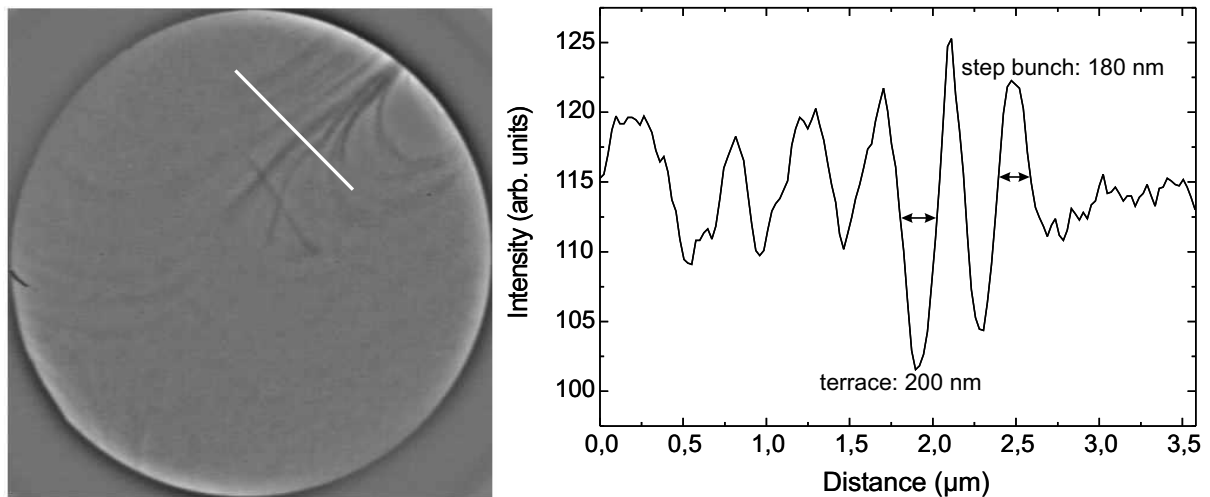


# 3 Substrate preparation and ultrathin film growth

The growth of Ni, Fe and Fe/Ni films on Cu(100) and their investigations by SPLEEM, XMCD and SQUID, respectively, have been performed in three different UHV-chambers. In all three cases cylindrical Cu(100) single crystals of 2 mm thickness were used. The diameter of the substrates was 10 mm for the SPLEEM and XMCD measurements and 5 mm for the SQUID experiments. Additionally, a square-shaped GaAs(001) crystal served as a substrate for Fe monolayers during the SQUID measurements. In this chapter the preparation of the substrates and the growth of the  $3d$  transition metal films is described.

## 3.1 Preparation of the Cu(100) and GaAs(001) substrates

A carefully developed substrate cleaning procedure was used to prepare the Cu(100) single crystals for the SPLEEM experiments. It was found to be effective to suppress possible bunching of atomic steps. Suppression of step bunching in substrate surfaces is an important issue in magnetic microstructure research, because even in otherwise highly perfect epitaxial ultrathin films, substrate step bunches can easily act as pinning sites for magnetic domain walls and thus influence the magnetic properties of the sample. Before each experiment, the Cu(100) crystal was prepared by 12 hours of  $\text{Ar}^+$ -ion sputtering, using a low current density of approximately  $0.1 \mu\text{A}/\text{cm}^2$  and an ion energy in the range of 1.5 – 3 keV. In order to heal up the imperfection and the roughness of the surface caused by the  $\text{Ar}^+$ -ion bombardment, the crystal was automatically flash annealed to about 1000 K in 10-minute intervals during sputtering. A previous investigation on the effects of ion bombardment and thermal treatment on the topography of Cu(001) surfaces revealed, that the average size of terraces is determined by the annealing temperature and not by the ion energy. The largest average size of terraces was found for the highest temperature (900 K) [166]. After this preparation schedule, no surface contamination was detectable using a single-pass cylindrical mirror Auger electron spectrometer (CMA). Imaging the bare Cu(100) substrate in the LEEM mode, we confirmed that the resulting surface had atomically flat terraces separated by mostly monoatomic steps. A typical prepared Cu(100) surface



**Figure 3.1:** Left: LEEM image of the sputtered and annealed Cu(100) crystal surface taken at an energy of the electrons of 9.5 eV. The dark lines are monoatomic step edges and step bunches separating different terraces. The field of view is 10  $\mu\text{m}$ . Right: Profile plot along the white line in the LEEM image. The average terrace width is  $\approx 200$  nm.

is depicted in the left image of Fig. 3.1, which shows Cu-step edges as dark lines by means of LEEM. A profile scan (right) across the white line in the left image reveals an average width of the Cu-terraces of  $\approx 200$  nm. Note, that the energy of the electrons was optimized for magnetic contrast of Ni, which occurs at 9.5 eV, and which may not be optimum to image structural features like Cu-step edges with highest contrast. Consequently, it cannot be ruled out that there are steps of atomic height –between the step bunches– which are not resolved. These would reduce the average width of the terraces.

Prior to the film growth for the XMCD measurements the cleanliness of the sputtered and annealed Cu(100) crystal was checked by x-ray absorption spectroscopy (XAS). The Cu(100) surface was cleaned until no contamination was detected in the x-ray absorption spectra, which otherwise reveal residual contaminations element-selectively. In the chamber, where the XMCD measurements have been performed, no Auger electron spectrometer was available.

The cleanliness of the Cu(100) and GaAs(001) substrates, on which Fe monolayers have been grown for the SQUID measurements, was checked by Auger electron spectroscopy. The cycles of sputtering and annealing were repeated until no residual contaminations of oxygen, carbon, carbon oxide or ferromagnetic materials from previous evaporations were detected by the CMA. A typical Auger spectrum of the bare Cu(100) crystal is shown in Fig. 3.2. The peaks in the spectrum are clearly identified as peaks originating from copper. No oxygen ( $E = 510$  eV) is detected.

In order to prepare the surface of the GaAs(001) crystal we followed the procedure described in Refs. [167,168], i.e. cycles of  $\text{Ar}^+$ -ion sputtering ( $E = 0.5 - 1$  keV) and annealing

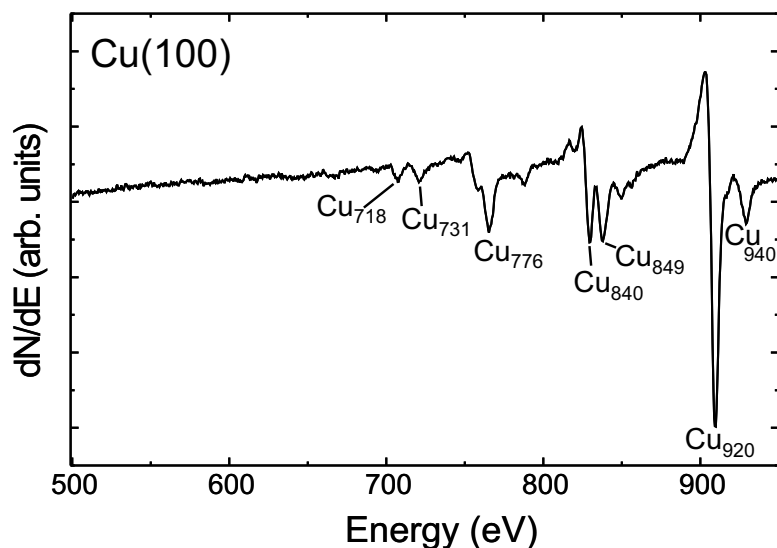


**Figure 3.2:** Auger spectrum of the bare Cu(100) crystal. No oxygen ( $E = 510$  eV) is detected.

(873 K), and a subsequent annealing at 873 K for 12 hours.

### 3.2 Growth of ultrathin Ni, Fe and Fe/Ni films on Cu(100) and GaAs(001)

Ni films were deposited *in situ* with the Cu(100) substrate held at either 100 K or 300 K. The evaporator target was a high purity rod of 2 mm diameter, which was brought to sublimation temperature by direct electron beam heating inside a water-cooled evaporator. The base pressure during SPLEEM measurements was  $2 \times 10^{-8}$  Pa; the maximum pressure during evaporation reached  $4 \times 10^{-8}$  Pa. The Ni evaporator has been calibrated before by growing a Ni/Cu(100) film at 300 K. The oscillation of the sum  $I^\uparrow + I^\downarrow$  of the average LEEM intensities as a function of the deposition time was used to observe the layer-by-layer growth of Ni/Cu(100) and to determine the layer thickness during the film growth as described elsewhere [169]. Since LEEM imaging of crystalline surfaces is based upon diffraction, and since the sum of the intensities  $I^\uparrow + I^\downarrow$  contains only diffraction information and no magnetic information, the well-known diffraction intensity oscillations [170] correspond to periodic nucleation, growth and completion of atomic monolayers during epitaxial growth. This oscillation is shown in Fig. 3.3. The distance between two maxima yields the Ni deposition rate, which was typically around 0.4 ML/min. The reduced amplitude of each following maximum (minimum) is attributed to roughness effects, which increase with the increasing number of atomic layers and have already been investigated [171, 172]. The oscillation disappears after 3 ML Ni in Fig. 3.3, which indicates a change of the layer-by-layer growth. Scanning tunnelling microscopy (STM) measurements showed a layer-by-layer growth of Ni/Cu(001) up to 5 ML, followed by a growth of pyramids with their  $\approx 6$  nm wide basis parallel to the  $\langle 110 \rangle$  directions. The STM images of a 9 ML Ni/Cu(001) revealed

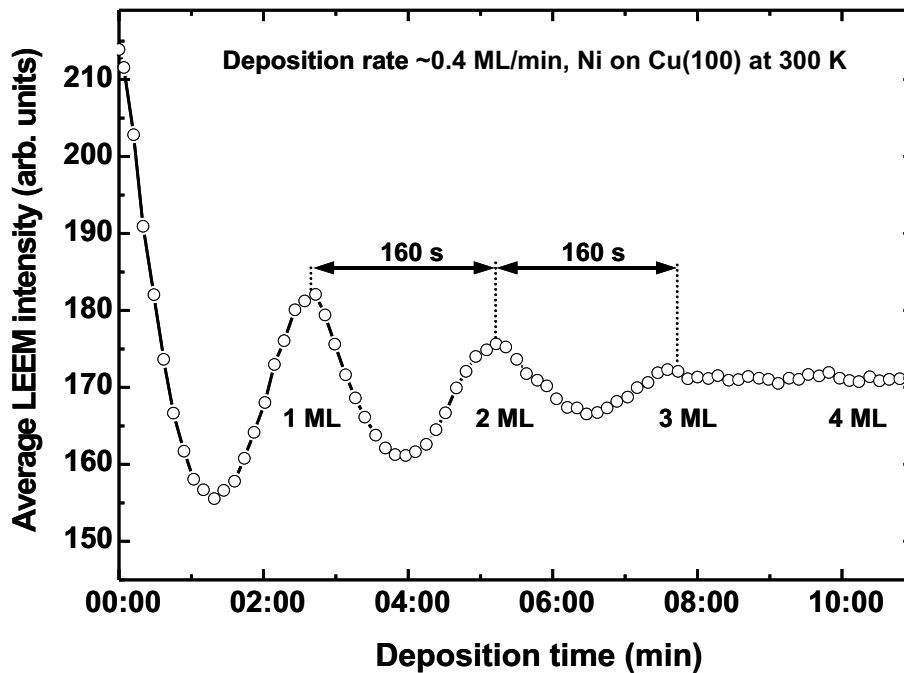


**Figure 3.3:** Film thickness calibration by the oscillation of the integrated LEEM intensity during the Ni deposition at 300 K. The maxima indicate full atomic Ni layers, and their distance determines the deposition rate equal to  $\approx 0.4$  ML/min. Each point corresponds to the sum of two  $\uparrow$ - and  $\downarrow$ -LEEM images.

3–4 unfinished layers [173]. Films grown at 100 K show a reduced amplitude and a faster decay of the intensity oscillation indicating a higher degree of roughness (not shown here). Since Ni/Cu(100) grows pseudomorphically up to thicknesses of about 15 ML [82,174], yielding a Ni(100) surface with the Cu lattice constant, Fe is expected to grow in a similar fct-like distorted structure on this Ni surface as on the blank Cu(100) surface. Fe films<sup>1</sup> have been grown on Ni/Cu(100) films with a deposition rate of typically 0.1 ML/min. This deposition rate, which is four times lower than that used for the 7 – 11 ML Ni/Cu(100) films, was chosen in order to precisely increase the Fe thickness near the SRT.

During the *in situ* XMCD investigation the thickness of Ni and Fe layers on Cu(100) was determined from the absorption spectra by using the edge-jump ratio  $J_R$ , which is the signal-to-background ratio at the  $L_3$  absorption edge. It is a precise measure for the number of emitted Auger electrons. From the calibration curve given in Ref. [154], in which  $J_R$  is plotted versus the layer thickness measured by a quartz micro balance, the layer thickness can be determined within an error of 0.25 ML for thicknesses below 3 ML. In the saturation range of the curve, i. e. around 20 ML thickness, the error becomes approximately 15%.

<sup>1</sup>The Fe evaporator was calibrated in the same way as the Ni evaporator, i. e. by the LEEM intensity oscillation at 300 K.

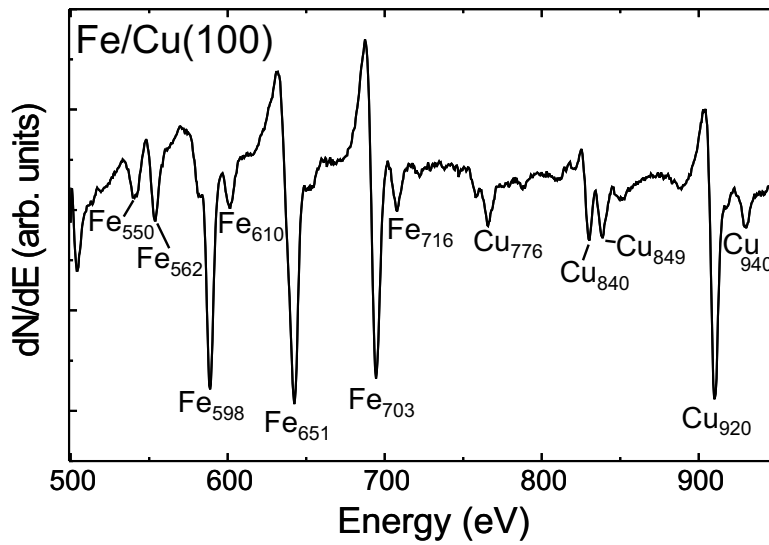


**Figure 3.4:** Auger spectrum of an Fe/Cu(100) film. From this spectrum the Fe thickness is determined by the calibration curve shown in the appendix A.5 in Fig. A.7 to be 4 ML.

For the purpose of controlled Fe film growth for SQUID measurements a careful thickness calibration of the Fe evaporator was performed. Therefore, Auger electron spectra of various Fe layer thicknesses on Cu(100) were taken. By the determination of the peak-to-peak signals of the Auger spectra of Cu at 920 eV and Fe at 651 eV and assigning the intensity ratios  $I_{\text{Cu}920}/I_{\text{Fe}651}$  to the different Fe layer thicknesses of the respective ratios from Ref. [175], a calibration curve of the Fe evaporator has been established. In Ref. [175] Auger spectra have been recorded at various Fe layer thicknesses, which have been determined by a quartz micro balance. The calibration curve is depicted in the appendix A.5 in Fig. A.7 and yields the correlation between the ratio of the Auger peak intensity and the Fe layer thickness and time of evaporation, respectively. From this curve the thickness of the Fe/Cu(100) film, whose CMA spectrum is displayed in Fig. 3.4, is determined to be 4 ML. The error of this thickness determination is estimated to be on the order of 20%. Unlike the CMA spectrum of the bare Cu(100) surface after cycles of cleaning (Fig. 3.2), the CMA spectrum of the 4 ML Fe/Cu(100) film clearly reveals traces of oxygen, which is indicated by the peak at an energy of 510 eV in Fig. 3.4. Comparing the low energy electron diffraction (LEED) images of the bare Cu(100) crystal and the Fe/Cu(100) film confirms the existence of oxygen atoms at the Fe surface. This

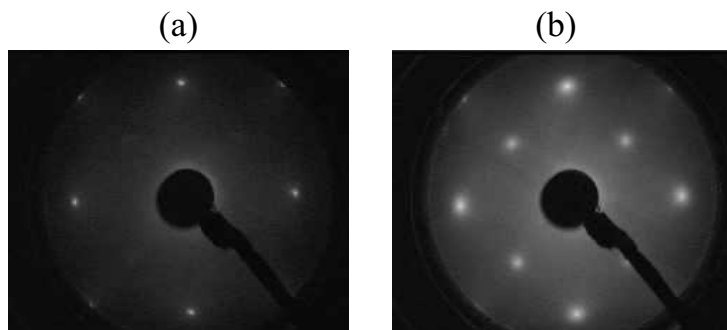


**Figure 3.5:** (a) LEED image of the bare Cu(100) crystal. (b) Crystallographic structure of a 4 ML Fe/Cu(100) film showing an oxygen superstructure. Both images have been taken at an energy of the electrons of 122 eV.

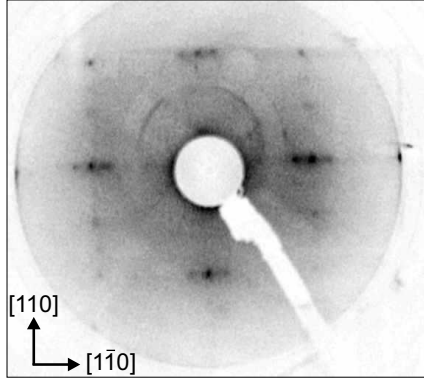


**Figure 3.6:** LEED image of the bare GaAs(001) substrate taken at an energy of the electrons of 127 eV at 300 K. The  $[1\bar{1}0]$  direction is parallel to the easy axis of the magnetization and parallel to the scan direction  $x$  during SQUID measurements.

is illustrated in Fig. 3.5. The Cu(100) surface (a) imaged at an energy of the electrons of 122 eV shows sharp  $1 \times 1$  LEED reflexes and a low background intensity, which is indicative for a low roughness. Higher degrees of roughness would lead to a diffuse scattering.

At the same energy of the electrons the Fe/Cu(100) film reveals additional spots originating from the oxygen atoms forming a  $2 \times 2$  superstructure. Moreover, the LEED pattern is more diffuse and the background intensity is higher as compared with the pattern of the bare substrate surface. This implies that the roughness of the Fe surface is much higher than the surface of the substrate. The existence of oxygen on the film and the rise in pressure up to  $1 \times 10^{-7}$  Pa during the evaporation indicates, that the Fe evaporator was not sufficiently degassed.

In preparation for SQUID measurements of ultrathin Fe/GaAs(001) films, square-shaped Fe films of an area of  $3 \times 3 \text{ mm}^2$  were grown on the cleaned GaAs(001) substrate using an aperture plate (see section 4.4). The distance between the crystal surface and the aperture was kept at a minimum distance below  $\approx 0.5 \text{ mm}$ , in order to evaporate films of sharp rectangular shape. This is important, since the simulation function of the magnetic stray field (section 2.3.2) is based on a perfectly rectangular thin film. Deviations from the rectangular shape will otherwise add errors in the determination of the magnetization.

Bcc Fe is known to grow epitaxial on GaAs(100) ‘with the film crystallographic axes coincident with those of the substrate’ [176]. At least between 5 ML and 30 ML Fe/GaAs(100) films exhibit a uniaxial in-plane magnetic anisotropy along the  $[0\bar{1}1]$  direction, which dominates over the fourfold bulk anisotropy along the  $[001]$  and  $[010]$  direction, respectively [177]. The resulting easy in-plane direction of the magnetization was found to be parallel to the  $[0\bar{1}1]$  axis. In Fig. 3.6 the LEEM image of the bare GaAs(001) substrate taken at an energy of the electrons of 127 eV is shown. The  $[1\bar{1}0]$  direction is parallel to the easy axis of the magnetization and parallel to the scan direction  $x$  during the SQUID measurements. By comparing the LEED images taken at different energies of the electrons, a  $4 \times 6$  reconstructed surface is revealed as was proposed by Xue *et al.* [178] on the basis of STM studies of GaAs(001).